Healing of Broken Multiwalled Carbon Nanotubes Using Very Low Energy Electrons in SEM: A Route Toward Complete Recovery

Neha Kulshrestha,[†] Abhishek Misra,[‡] Kiran Shankar Hazra,[†] Soumyendu Roy,[†] Reeti Bajpai,[†] Dipti Ranjan Mohapatra,[†] and D. S. Misra[†,*]

[†]Department of Physics and [‡]Department of Electrical Engineering, Indian Institute of Technology Bombay, Mumbai 400076, India

ABSTRACT We report the healing of electrically broken multiwalled carbon nanotubes (MWNTs) using very low energy electrons (3−10 keV) in scanning electron microscopy (SEM). Current-induced breakdown caused by Joule heating has been achieved by applying suitably high voltages. The broken tubes were examined and exposed to electrons of 3−10 keV *in situ* in SEM with careful maneuvering of the electron beam at the broken site, which results in the mechanical joining of the tube. Electrical recovery of the same tube has been confirmed by performing the current−voltage measurements after joining. This easy approach is directly applicable for the repairing of carbon nanotubes incorporated in ready devices, such as in on-chip horizontal interconnects or on-tip probing applications, such as in scanning tunneling microscopy.

KEYWORDS: carbon nanotubes · electron irradiation · *I*−*V* characteristics · interconnects · Joule heating

Experimental and theoretical studies on multiwalled carbon nanotubes (MWNTs) have suggested their peerless electrical properties, such as high electrical conductivity and extraordinary current carrying capacity (10^8−10^9 A/cm^2),[1,2] and paved the way to imagine ultrafast nanoelectronic circuits with their use as on-chip interconnects. However, ultimately, all this is limited by Joule heating as it leads to the breakdown of the tube. Several experiments carried out so far for the electrical characterization of the MWNTs suggest the breaking of the tube due to Joule heating after the application of a certain voltage.[3−5] We here suggest that a very low energy electron beam may be beneficial to repairing such breakages. The effect of high-energy ion (megaelectronvolt range)[6,7] or high-energy electron beam (100−200 keV range) irradiation has been reported in several studies to result in amorphization, bending, kinking, cutting, or deformation of the tube.[8] The welding or soldering of the intertube junctions has also been reported in the literature.[9−11] In a very important study by Banhart, the connection between the surfaces of two crossing carbon nanotubes has been made by electron irradiation.[9] However, the electrical characterization of the so-formed junction has not been performed. In another interesting study,[11] the use of a mechanical manipulator in transmission electron microscopy (TEM) made possible the interconnections of carbon nanotubes. However, the sample requirements for TEM studies are different; hence, studies done in TEM are less feasible from their application point of view. Furthermore, the *I*−*V* measurements in TEM involve the contact of some protruding CNTs with a metal tip or probe, and not all the TEM systems are equipped with such sophisticated facilities. There is a lack of experiments with *ex situ* post-*I*−*V* measurements to investigate the electrical transport through such nanoengineered systems. In this study, healing of the broken CNTs by very low energy electrons in scanning electron microscopy (SEM) without connecting them by a mechanical manipulator and *ex situ* post-healing *I*−*V* measurements proves it as an easy and more feasible approach for applications.

In this paper, we demonstrate the rejoining of a single MWNT broken due to the Joule heating during the *I*−*V* analysis. This has been achieved by exposing the broken ends of the tube to very low energy electrons (3−10 keV) in SEM. Under the electron beam, the broken ends of the tube swell and time evolution of this rejoining phenomenon has been consistently observed during SEM imaging. Further *I*−*V* measurements on the as-repaired tube were obtained to confirm the electrical rejoining. We have noticed that, although the amount

*Address correspondence to drk1955@gmail.com.

Received for review September 5, 2010 and accepted January 30, 2011.

Published online February 23, 2011
10.1021/nn102288u

of current in postjoining $I-V$ measurements may be significantly low, nevertheless, it is important that this current can be improved by some treatments, such as current-induced annealing. The lithographic approach to fabricate and characterize the nanotube device with the extensive use of microscopy without the use of any mechanical manipulator involved and *ex situ* electrical measurements at every step ensures the uniqueness of our experiments in terms of their repeatability and reliability.

RESULTS AND DISCUSSION

The SEM image of the oriented pillars of multiwalled nanotubes grown at lithographically defined circles of SiO_2 with a diameter of 9 μm with a 4 μm spacing between them is shown in Figure 1a, and the Raman spectra of the same sample is shown in Figure 1b. The two peaks obtained at 1344 and 1567 cm^{-1} are two well-known features in the Raman spectra of the MWNT literature and are termed as the D-band and the G-band, respectively.[12] The ratio of the intensity of the D-peak to G-peak (I_D/I_G), that is, the ratio of defects or disorders, such as the presence of amorphous carbon to crystalline sp^2 amount, obtained from this spectra is 0.88, which suggests that as-deposited CNTs have few defects and little amorphous carbon content.

One advantage of using the CNTs from pillars is that, as the CNTs grow vertically in pillars, it is rather easy to separate them as compared to the otherwise grown CNTs, such as in films or mats grown by microwave plasma chemical vapor deposition (MPCVD) or thermal CVD. Moreover, the CNTs in pillars are less entangled than they are in films or mats and their average length is more as the pillars can grow vertically up to millimeter size depending on the growth parameters, such as growth time. Even after ultasonication for several times, the tube length remains sufficient for their further use, especially for the purpose where the length of the tubes is important to cross or bridge the structures, such as in $I-V$ measurements. We have used the CNTs from the pillars grown up to a height of 50 μm; however, the length of the tubes becomes short after ultasonication.

Figure 2a shows the SEM image of an individual MWNT spanning the gap between two gold pads. The $I-V$ characteristic of the same tube is shown in Figure 2b. The current reached up to 140 μA as the voltage was swept up to 3.0 V. The resistance obtained from this graph is 21.4 kΩ, which is in accordance with the typical resistance values of an MWNT in a two-probe configuration.[13,14] It is worth noticing that, for these measurements, no treatments, such as thermal or electrical annealing, have been done to improve the metal−nanotube contact, which lowers the contact resistance. The maximum current density for this tube is of the order of 10^7 A/cm^2, hence comparable to the current density of the tubes in the work reported by Lee *et al.*[14]

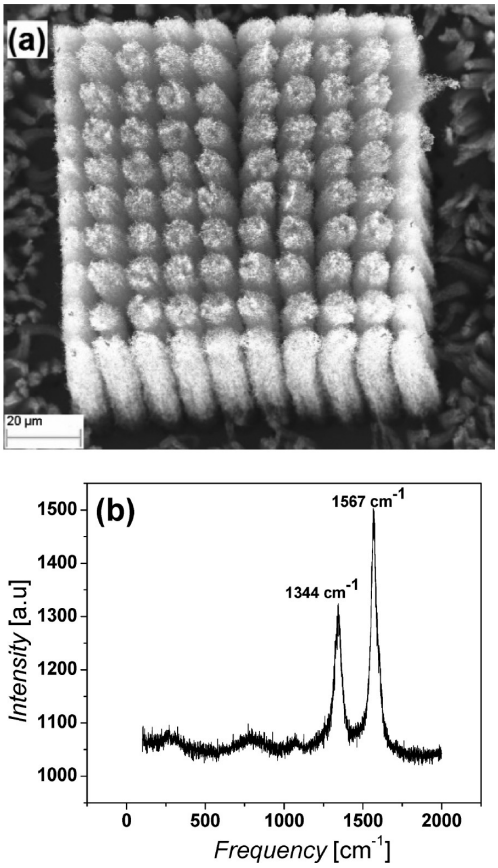

Figure 1. (a) SEM image of the as-grown MWNT pillars. (b) Raman spectra of the as-grown MWNT.

As the voltage was applied beyond 4 V, the $I-V$ characteristic obtained was just the noise oscillating almost around a zero value of current, indicating the breakdown of the tube, as shown in Figure 2e. The breakdown of the tube has been confirmed by the SEM imaging, as shown in Figure 2c. Thinning at the broken site of the tube (diameter = 33.25 nm) in the SEM image combined with $I-V$ observations suggests that the tube has been broken abruptly by simultaneous oxidation of multiple shells induced by Joule heating. During SEM imaging, a prominent swelling of the broken ends of the tube has been noticed as the electron beam with an energy of 10 keV was focused at this broken area, and with a continuous increment in size, the two ends finally coalesce, as shown in Figure 2d. After swelling and rejoining, the diameter of the tube at the local site becomes 65.38 nm, which is almost double as compared with the diameter of the tube at this site just before healing. Such rejoining of the tube is interesting in the wake that no manipulation has been employed to move the two ends toward each other. Further investigation suggests that the deposition of amorphous carbon is responsible for the swelling that appears because of the change in the diameter of the tube at the particular site of focusing, as presented later in this paper.

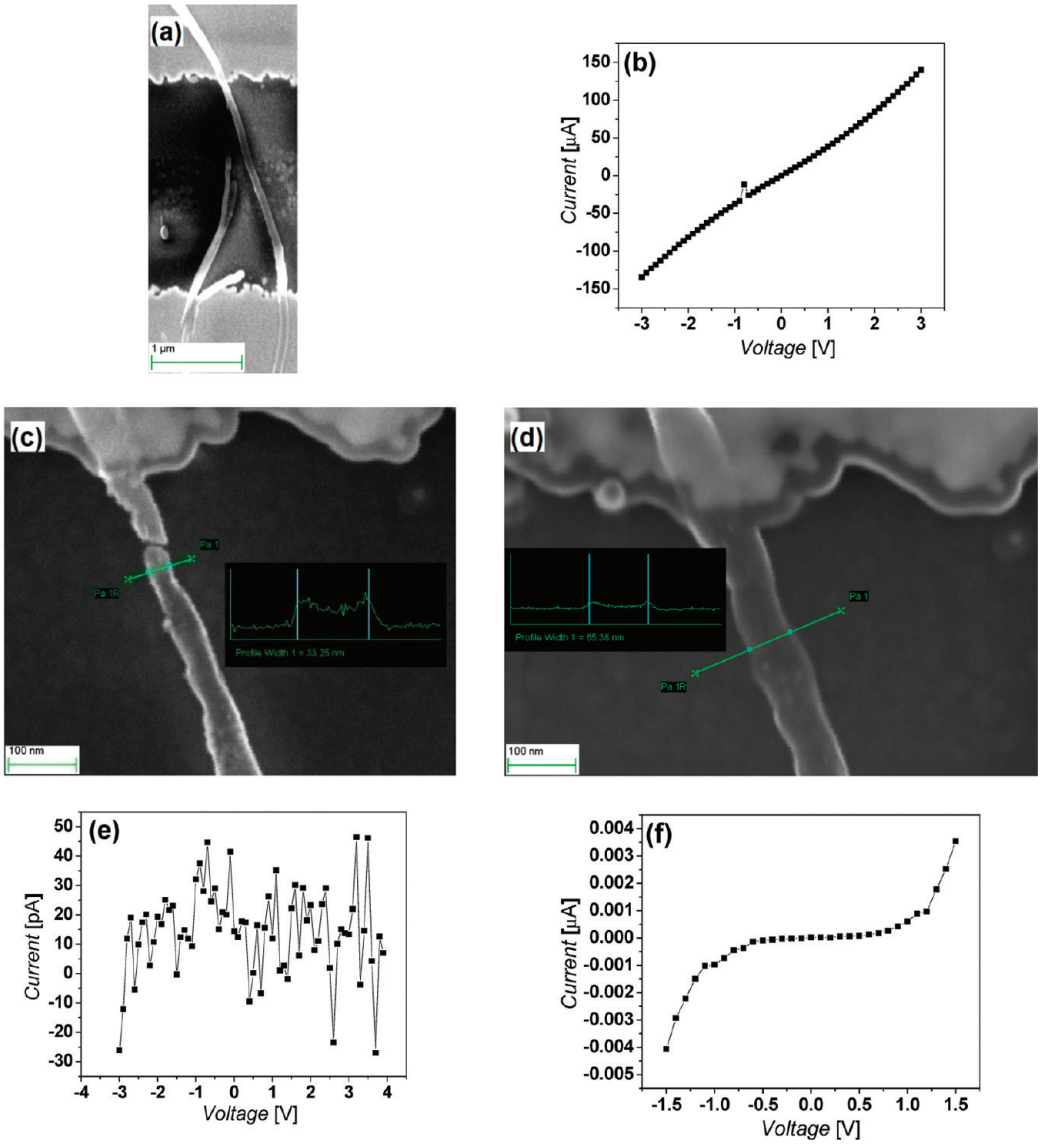

Figure 2. (a) MWNT between two gold pads. (b) *I*−*V* characteristic of the tube shown in (a). (c) Broken MWNT after *I*−*V* measurements. (d) The same tube after healing in SEM. (e) *I*−*V* characteristic of the tube after breakdown. (f) *I*−*V* characteristic of the tube after joining.

One step ahead, we measured the *I*−*V* characteristic of the as-repaired tube and found very less, but not negligible, current, as shown in Figure 2f, hence reflecting the electrical joining of the tube. The degradation of the current after joining is due to the structural changes in the tube at and around the irradiated area of the tube. To confirm the healing effect and electrical joining, the same experiment has been carried out on different tubes. In these experiments, we noticed that, by gradual current-induced annealing, that is, first applying the low voltages and then gradually increasing the voltage range, the *I*−*V* curves of the tube and its resistance after joining can be substantially improved. This current-induced annealing has been reported in some other studies as well.[11,15] The SEM image of another MWNT is shown in Figure 3a. For contact improvement, this time current annealing has been employed, and a clear improvement in current has been observed, as shown in Figure 4a, and voltage sweeps were applied until the breakdown of the tube. The *I*−*V* characteristic up to the voltage range of −6 to +6 V for this tube before breaking down is also shown in the same Figure 4a. Beyond this voltage range, the *I*−*V* curve was very similar to that shown in Figure 2e, indicating the breakdown of the tube. Again, the healing effect of the tube has been confirmed in SEM with 10 keV electrons, and the time evolution of the healing of the tube is shown in Figure 3c. In fact, this image (Figure 3c) of the tube has been taken after 1 min of electron irradiation at the broken site. After 2 min, the complete healing of the tube is clearly visible, as shown in Figure 3d. The same effect of healing was also visible for other broken tubes with 3 keV

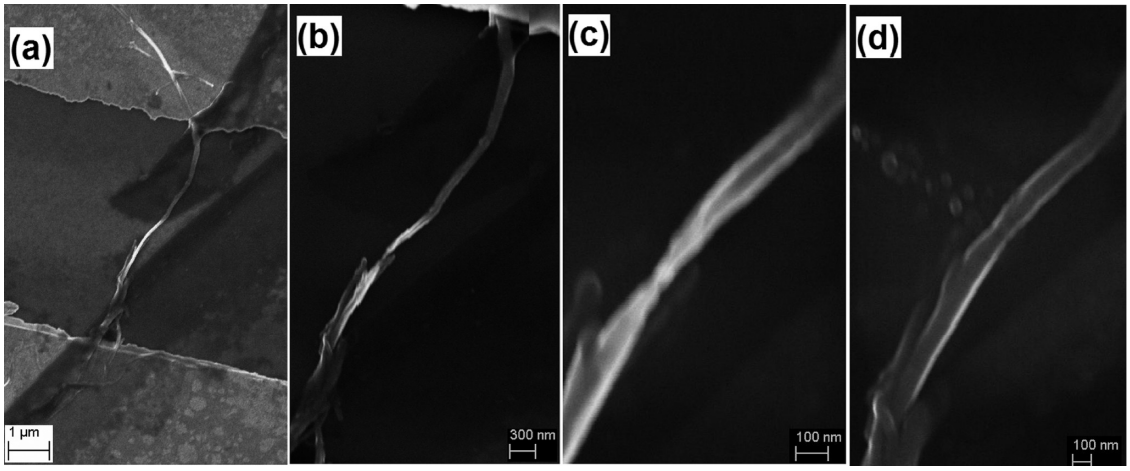

Figure 3. (a) MWNT between two gold pads. (b) After complete breakdown. (c) MWNT during rejoining. (d) MWNT after complete joining.

electrons, but with more time involved in the process because of a lower rate of amorphous carbon deposition. It is worth pointing out that, although, in this study, the electron energies used are from 3 to 10 keV, the similar results are expected with the electron energies of less than 100 keV. However, the energies higher than 100 keV can cause damage to the tubes rather than healing by knock on collisions.[16] After healing, the $I-V$ characteristics of the same tube have been again obtained in order to confirm the electrical joining. In this experiment, however, the tube has been annealed by repeated current measurements in all voltage ranges up to 6 V, as shown in Figure 4b. The effect of current annealing on the resistance of the tube between various voltage ranges is tabulated in Table 1 before and after joining. It was found that the current increases and becomes almost similar to the current before the breakdown of the tube in the voltage range of −5 to 5 V, as is clear from Figure 4c. However, the $I-V$ characteristic in the voltage range of −6 to +6 V after repairing indicated that the current value is substantially decreased after 5 V, suggesting that the tube is approaching toward breakdown as the voltage range increases. For comparison, the $I-V$ characteristic of the tube in the voltage range of −6 to 6 V, before breakdown and after healing, is shown in Figure 4d. In this experiment, the improvement in the current behavior as a result of current annealing (before and after breakdown of the tube) is clearly visible as compared to the previous tube (tube 1), where no current annealing has been employed. The most possible explanation of the joining, as suggested in other studies too,[9,11] is the deposition of amorphous carbon at the junction, which is attributed to the electron-beam-induced deposition (EBID). In this process, the hydrocarbon molecules that are present as the source of contamination in the vacuum of the microscope are dissociated and deposited by the electron beam at the spot of focusing. The change in the $I-V$ behavior of the tube and hence in its electrical resistance after electron irradiation is performed to rejoin the two broken ends of the CNT is due to the presence of the amorphous carbon content at the particular site of focusing. With these changes occurring at the junction after electron irradiation, the mobility of electrons also changes, leading to the degradation in current after joining. However, current-induced annealing may lead to the graphitization at the junction and current values are substantially improved by taking several current sweeps.

To investigate the physical phenomena taking place at the broken site after healing by such low-energy (3−10 keV) electrons in SEM, the high-resolution transmission electron microscopy (HRTEM) and X-ray photoelectron spectroscopy have been carried out.

High-Resolution Transmission Electron Microscopy (HRTEM) Analysis. The presence of amorphous carbon at the junction has been confirmed by the HRTEM observation. For this experiment, MWNTs from the same sample were dispersed on a copper mesh TEM grid and irradiated at the same conditions in SEM and were carefully located for their HRTEM investigation. The SEM image of the tube before and after irradiation is shown in Figure 5a,b, respectively. In Figure 5b, the arrow indicates the irradiated region of the tube. HRTEM images of the same irradiated area are shown in Figure 6a−e at subsequently higher magnifications. The deposition of amorphous carbon around the tube is clearly visible from the images. Hence, our study demonstrates that such low-energy electrons (3−10 keV) in very common SEM systems are useful for the repairing and one does not need to go for higher-energy electrons or complex sample preparations, such as in the case of TEM.

X-ray Photoelectron Spectroscopy Analysis. The XPS measurements, carried out with a Thermo VG Scientific Multilab 2000 photoelectron spectrometer, also

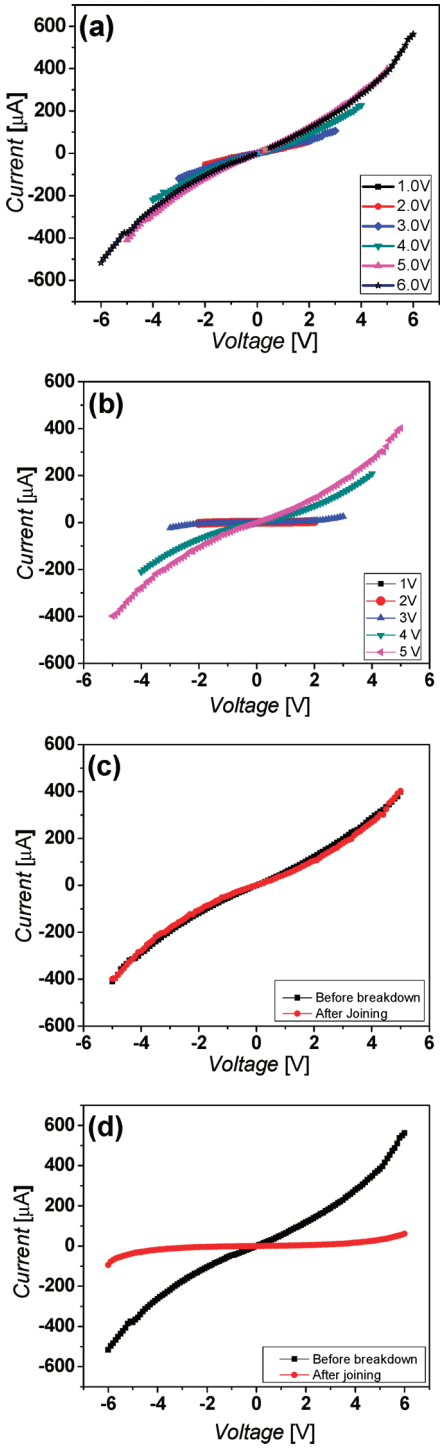

Figure 4. (a) *I*−*V* curve for the CNT shown in Figure 3a showing current annealing before the breakdown of tube. (b) *I*−*V* curve for the CNT shown in Figure 3d, after joining by e-irradiation in SEM. (c) Comparison of current values in the voltage range of −5 to 5 V, before and after joining. (d) Comparison of current values in the voltage range of −6 to 6 V, before and after joining.

confirm the presence of amorphous carbon at the junction as a result of electron irradiation. The Mg Kα radiation with a photon energy of 1253.6 eV is used as the excitation source. Carbon 1s core level spectra have been collected in the hemispherical analyzer. For the

TABLE 1. Showing the Effect of Current Annealing on the Resistance of Tube 2, Shown in Figure 3

voltage range	average resistance (kΩ) before breakdown	average resistance (kΩ) after joining
−0.5 to 0.5	48.3	2500
−1.0 to 1.0	43.2	1800
−2.0 to 2.0	37.7	1000
−3.0 to 3.0	26.8	435.5
−4.0 to 4.0	18.9	22.5
−5.0 to 5.0	13.7	15.2

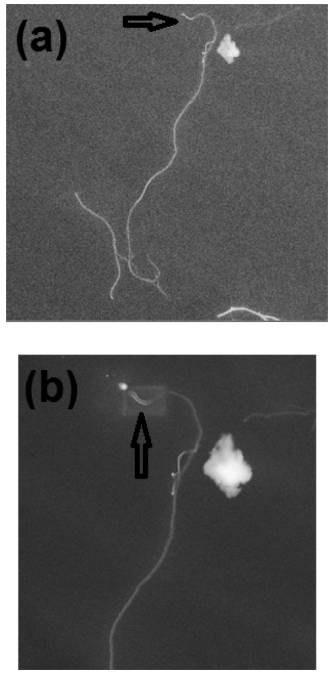

Figure 5. (a) SEM image of the MWNT before electron irradiation. (b) SEM image of the MWNT after electron irradiation. The arrow indicates the irradiated area.

XPS measurement, the sample was just the carbon nanotubes dispersed from pillars by the same technique as described earlier. However, this time the tubes were not individual, but in a large quantity. The XPS measurement was done both before and after the electron irradiation (for 10−15 min). Because the irradiated area was large, the time employed for irradiation has been kept long. However, the other parameters, such as accelerating voltage, working distance, *etc.*, in the SEM have been kept the same. The XPS spectra before and after electron irradiation are shown in Figure 7a,b, respectively. The spectrum is deconvoluted in two peaks. The peak at lower binding energy is assigned to the sp^2 peak, and the peak at higher binding energy is the sp^3 peak.[17−19] Hence, in Figure 7a,b, the peak at a binding energy of 284 eV corresponds to sp^2-bonded carbon atoms, which represents the graphitic nature of the carbon. Because the amorphous carbon is commonly considered as a mixture of sp^2 and sp^3 hybridized carbon atoms, the

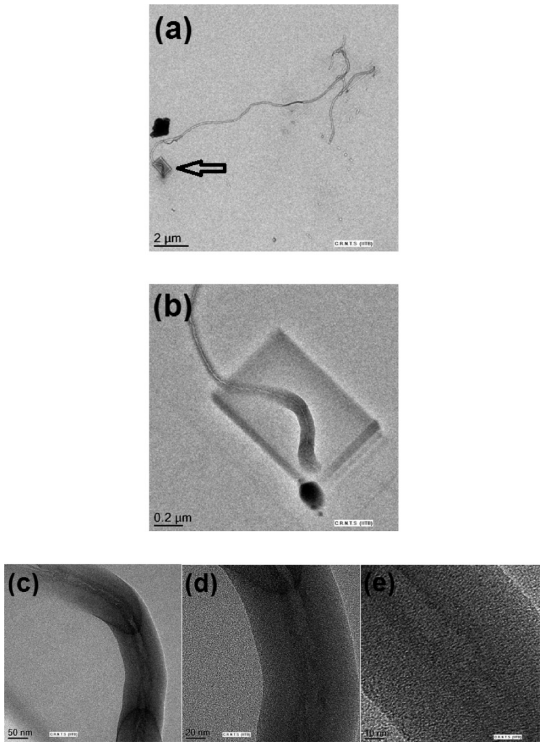

Figure 6. (a) TEM image of the MWNT after electron irradiation. The arrow indicates the irradiated area. (b) HRTEM image of the MWNT in the irradiated area at higher magnification. (c–e) HRTEM images of the MWNT in the irradiated area at sequentially higher magnifications.

peak at 285.5 eV may be assigned to amorphous carbon. After the electron irradiation, the increased area under the sp^3 peak, as is clear from Figure 7b, indicates the increased amount of amorphous carbon in the sample.

To summarize the results presented in this paper, the joining of electrically broken multiwalled carbon nanotubes in scanning electron microscopy has been shown by a very mild electron irradiation of 10 keV in energy. Deliberate exposure of the broken ends of the tube for about 2 min to the electron beam with an energy of 3–10 keV results in the joining of the tube. However, the exact time to ensure the healing depends on the amount of breakage caused by the Joule heating and the electron energies used. We suggest that exposing the broken ends of an MWNT to an

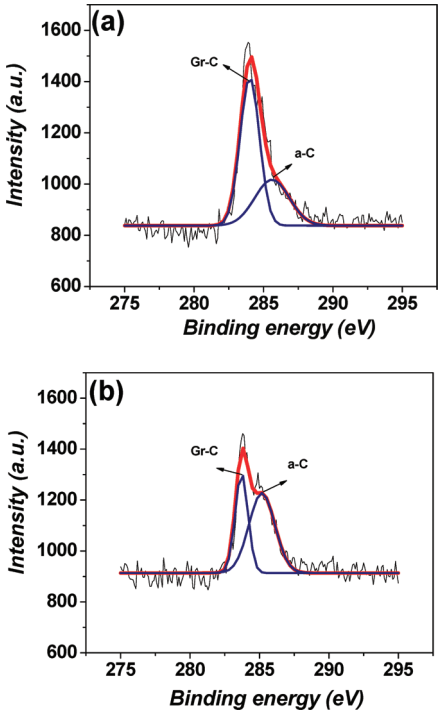

Figure 7. (a) XPS spectra of the CNT sample before electron irradiation. (b) XPS spectra of the CNT sample after electron irradiation.

electron beam during SEM leads to the mechanical joining of the tubes and that they can also be electrically repaired to a great extent, as confirmed by electrical measurements after healing. We have also shown that almost complete mechanical and electrical recovery of the tube may be obtained by employing current annealing with the resistance being almost similar to the resistance of the tube before breaking down. Our results of mechanical as well as electrical joining of the tubes are important in various applications of the repairing of CNTs, such as where they are attached with some tip for probing or in electrical circuits. The insight of the phenomena occurring at the so-produced junctions may be interesting to developing some new applications; for example, diode-like behavior may be obtained combining two differently doped CNTs.

EXPERIMENTAL DETAILS

Multiwalled carbon nanotubes used for our experimental purpose were synthesized by thermal chemical vapor deposition using a ferrocene–toluene mixture as the precursor. To grow nanotubes vertically in the pillar form at the pattern sites, first, a silicon oxide layer with a thickness of 100 nm was grown on a 2 in. p-type silicon wafer. A chromium–gold layer with a total thickness of 150 nm was then sputtered on the wafer. For the circular dots of SiO_2 separated by Cr/Au, a pattern was made using Klevin software and a mask was written by a laser writer. Using a photolithography technique, the mask was transferred on the wafer. Using wet etching, the Cr–Au was then removed to get cirular dots of SiO_2 patterned at the wafer. The so-obtained wafers were used as a substrate for the growth of the tubes in thermal CVD. In the thermal CVD apparatus, the mixture of ferrocene and toluene (0.1 g of the former in 5 mL of the latter) was injected into the heating zone of the furnace at a temperature of 800 °C. A flow of 75 sccm carrier gas (hydrogen) was maintained during the growth.

Patterns for contact pads were directly written using electron beam lithography on the predeposited Cr–Au layer with a total thickness of around 250 nm with dielectric silicon dioxide with a

thickness of 200 nm beneath them. Using wet etching of Cr/Au, a spacing of 3−4 μm between the pads was fixed. Carbon nanotubes were transferred on the so-achieved patterns in order to have them suspended between the two random pads. These nanotubes were examined using scanning electron microscopy. A Raith-150 TWO high-resolution SEM apparatus was used for this purpose. Positions of gold pads on the substrate and nanotubes on the gold pads were fixed and noted down carefully for the further steps. Current−voltage characteristics of these individual tubes were obtained using a Keithley 4200 source meter and Proxima probe station using a two-probe configuration. A control program (for two-D resistive wire) facilitated to sweep the voltages up to the predefined voltage with desired steps and corresponding current values. Successive voltage sweeps were applied for sequentially higher ranges in order to achieve the current-induced breakdown.

Acknowledgment. We acknowledge Prof. Anil Kottantharayil, Prof. R. Pinto, and Prof. Souvik Mahapatra of the Centre for Excellence in Nanoelectronics (CEN), Dept. of Electrical Engineering, IITB, for providing the help in SEM imaging, lithography, and electrical measurements. We also acknowledge the Sophisticated Analytical Instrument facility (SAIF), IITB, for providing the HRTEM facility.

REFERENCES AND NOTES

1. Wei, B. Q.; Vajtai, R.; Ajayan, P. M. Reliability and Current Carrying Capacity of Carbon Nanotubes. *Appl. Phys. Lett.* **2001,** *79*, 1172–1174.
2. Kreupl, F.; Graham, A. P.; Liebau, M.; Duesberg, G. S.; Seidel, R.; Unger, E. Carbon Nanotubes for Interconnect Applications. *IEEE Int. Electron Devices Meet.* **2004,** 683–686.
3. Collins, P. G.; Arnold, M. S.; Avouris, P. Engineering Carbon Nanotubes and Nanotubes Circuits Using Electrical Breakdown. *Science* **2001,** *292*, 706–709.
4. Molhave, K.; Gudnason, S. B.; Pedersen, A. T.; Hyttel, C.; Horsewell, A.; Boggild, P. Transmission Electron Microscopy Study of Individual Carbon Nanotube Breakdown Caused by Joule Heating in Air. *Nano Lett.* **2006,** *6*, 1663–1668.
5. Tsutsui, M.; Taninouchi, Y. K.; Kurokawa, S.; Sakai, A. Electrical Breakdown of Short Multiwalled Carbon Nanotubes. *J. Appl. Phys.* **2006,** *100*, 094302.
6. Mathew, S.; Bhatta, U. M.; Ghatak, J.; Sekhar, B. R.; Dev, B. N. The Effects of 2 MeV Ag Ion Irradiation on Multiwalled Carbon Nanotubes. *Carbon* **2007,** *45*, 2659–2664.
7. Kim, H. M.; Kim, H. S.; Park, S. K.; Joo, J.; Lee, T. J.; Lee, C. J. Morphological Change of Multiwalled Carbon Nanotubes Through High-Energy (MeV) Ion Irradiation. *J. Appl. Phys.* **2005,** *97*, 0261039.
8. Kiang, C. H.; Goddard, W. A.; Beyers, R.; Bethune, D. S. Structural Modification of Single-Layer Carbon Nanotubes with an Electron Beam. *J. Phys. Chem.* **1996,** *100*, 3749–3752.
9. Banhart, F. The Formation of a Connection between Carbon Nanotubes in an Electron Beam. *Nano Lett.* **2001,** *1*, 329–332.
10. Terrones, M.; Banhart, F.; Grobert, N.; Charlier, J. C.; Terrones, H.; Ajayan, P. M. Molecular Junctions by Joining Single-Walled Carbon Nanotubes. *Phys. Rev. Lett.* **2002,** *89*, 075505.
11. Wang, M.; Wang, J.; Chen, Q.; Peng, L. M. Fabrication and Electrical and Mechanical Properties of Carbon Nanotube Interconnections. *Adv. Funct. Mater.* **2005,** *15*, 1825–1831.
12. Dresselhaus, M. S.; Dresselhaus, G.; Saito, R.; Jorio, A. Raman Spectroscopy of Carbon Nanotubes. *Phys. Rep.* **2005,** *409*, 47–99.
13. Kreupl, F.; Graham, A. P.; Duesber, G. S.; Steinhogl, W.; Liebau, M.; Unger, E.; Honlein, W. Carbon Nanotubes in Interconnect Applications. *Microelectron. Eng.* **2002,** *64*, 399–408.
14. Lee, S. B.; Teo, K. B. K.; Chhowalla, M.; Hasko, D. G.; Amaratunga, G. A. J.; Milne, W. I.; Ahmed, H. Study of Multi-Walled Carbon Nanotube Structures Fabricated by PMMA Suspended Dispersion. *Microelectron. Eng.* **2002,** *61−62*, 475–483.
15. Kitsuki, H.; Yamada, T.; Fabris, D.; Jameson, J. R.; Wilhite, P.; Suzuki, M.; Yang, C. Y. Length Dependence Of Current Induced Breakdown in Carbon Nanofiber Interconnects. *Appl. Phys. Lett.* **2008,** *92*, 173110.
16. Banhart, F. Irradiation Effects in Carbon Nanostructures. *Rep. Prog. Phys.* **1999,** *62*, 1181–1221.
17. Filik, J.; May, P. W.; Pearce, S. R. J.; Wild, R. K.; Hallam, K. R. XPS and Laser Raman Analysis of Hydrogenated Amorphous Carbon Films. *Diamond Relat. Mater.* **2003,** *12*, 974–978.
18. Leung, T. Y.; Man, W. F.; Lim, P. K.; Chan, W. C.; Gaspari, F.; Zukotynsky, S. Determination of the sp^3/sp^2 Ratio of a-C:H by XPS and XAES. *J. Non-Cryst. Solids* **1999,** *254*, 156–160.
19. Merel, P.; Tabbal, M.; Chaker, M.; Moisa, S.; Margot, J. Direct Evaluation of the sp^3 Content in Diamond-Like-Carbon Films by XPS. *Appl. Surf. Sci.* **1998,** *136*, 105–110.